Inorganic Chemistry

ARTICLE

pubs.acs.org/IC

Mechanistic and Computational Studies of the Atom Transfer Radical Addition of CCl_4 to Styrene Catalyzed by Copper Homoscorpionate Complexes

José María Muñoz-Molina,[†] W. M. C. Sameera,[‡] Eleuterio Álvarez,[§] Feliu Maseras,[∥,⊥] Tomás R. Belderrain,*[,†] and Pedro J. Pérez*[,†]

[†]Laboratorio de Catálisis Homogénea, Departamento de Química y Ciencia de los Materiales, Unidad Asociada al CSIC, Centro de Investigación en Química Sostenible (CIQSO), Universidad de Huelva, Campus de El Carmen, 21007 Huelva, Spain

[‡]Inorganic Chemistry Laboratory, Department of Chemistry, University of Oxford, South Parks Road, Oxford OX1 3QR, United Kingdom

[§]CSIC-Universidad de Sevilla, Avenida de Américo Vespucio, 49, 41092 Sevilla, Spain

[∥]Institute of Chemical Research of Catalonia (ICIQ), 43007 Tarragona, Catalonia, Spain

[⊥]Departament de Quimica, Universitat Autonoma de Barcelona, 08193 Bellaterra, Catalonia, Spain

Supporting Information

ABSTRACT: Experimental as well as theoretical studies have been carried out with the aim of elucidating the mechanism of the atom transfer radical addition (ATRA) of styrene and carbon tetrachloride with a $Tp^xCu(NCMe)$ complex as the catalyst precursor (Tp^x = hydrotrispyrazolyl−borate ligand). The studies shown herein demonstrate the effect of different variables in the kinetic behavior. A mechanistic proposal consistent with theoretical and experimental data is presented.

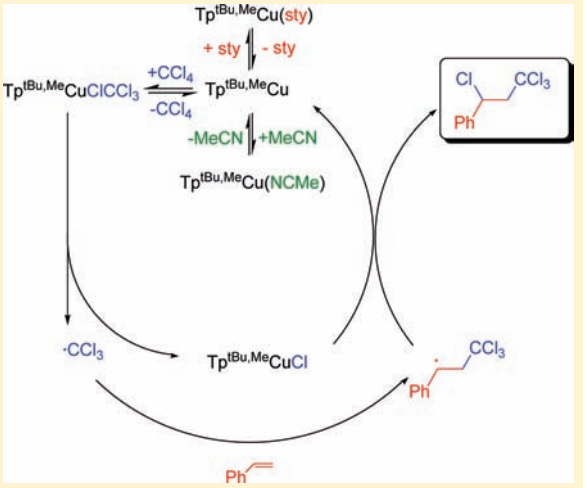

INTRODUCTION

The addition of a polyhalogenated saturated hydrocarbon to an olefin, namely, the Kharasch reaction, constitutes an efficient way to generate carbon−carbon bonds (Scheme 1a).[1] This reaction may occur in the presence either of a free-radical precursor as the halogen transfer agent or of a transition metal complex as the catalyst. In the latter case, the so-called atom transfer radical addition (ATRA) reaction,[2] the transformation has been explained in terms of three steps, two of which are metal-mediated. The first step proceeds via a metal-induced homolytic cleavage of the carbon−halogen bond, affording a metal−halide complex and a carbon-centered radical (activation step). Subsequently, the latter species interacts with the olefin to form a second radical species which induces the abstraction of halogen from the above metal−halide complex (deactivation step). Therefore, the metal center undergoes a reversible oxidation−reduction process, changing its oxidation state on one unit.

Several metals have been described to catalyze this transformation, which has been described in both the inter- and intramolecular versions.[2] Early work focused in ruthenium-[3] or nickel-based[4] catalysts showed very high activities for the intermolecular case, whereas the use of copper was restricted to the intramolecular atom transfer radical cyclization (ATRC) reaction.[2e] However, in the past decade the use of copper complexes as catalysts in the intermolecular reactions has emerged with excellent results.[2a] Thus, Pintauer and co-workers have reported the efficient ATRA of polyhalogenated alkanes to olefins such as 1-hexene

Received: November 13, 2010
Published: February 14, 2011

   dx.doi.org/10.1021/ic102279w | *Inorg. Chem.* 2011, 50, 2458–2467

Scheme 1. (a) Kharasch Reaction and (b−d) Commonly Proposed Mechanism for the Metal-Mediated Atom Transfer Radical Addition (ATRA) Reaction

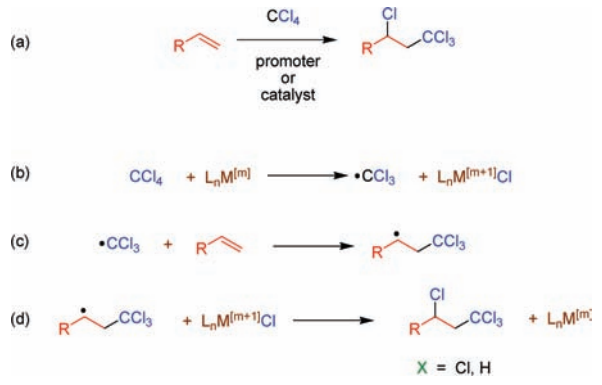

Scheme 2. Previous Mechanistic Proposal for ATRA Reactions Catalyzed by Tp^xCu Complexes

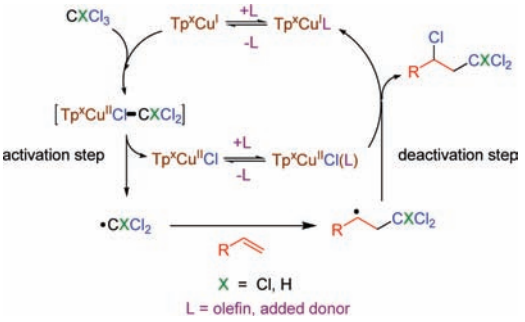

or 1-octene (with TONs as high as 160 000 with 5 ppm of catalyst loading).[5] Our group has recently described that copper−homoscorpionate complexes catalyze the atom transfer radical addition of polyhalogenated alkanes to terminal olefins[6] or to α,ω-dienes,[7] affording in the latter case five-membered carbocycles by a concurrent intramolecular radical process. Although the overall mechanism of this transformation has been accepted as that shown in Scheme 1, the intimate nature of the different steps as well as the effect of the different variables has not yet been fully described. In our first contribution in this area,[6b] we proposed a plausible mechanism for these ATRA reactions (Scheme 2) catalyzed by complexes Tp^xCu (Tp^x = hydrotrispyrazolylborate ligand) on the basis of kinetic data obtained. Since the knowledge of the mechanism would afford the design of more active catalysts, we have decided to carry out a complete mechanistic study on an ATRA model reaction, including experimental as well as theoretical calculations, using $Tp^{tBu,Me}Cu(NCMe)$ as the catalyst (**1**, Scheme 3). A complete mechanistic picture is now proposed that explains not only the route leading to the formation of the addition product but also the important role of all the reagents in the control of the catalyst precursor and therefore in the well-known persistent radical effect equilibrium,[2b] which is crucial for this transformation.

RESULTS AND DISCUSSION

Catalyst Precursor: Structure and Behavior in Solution. The complex $Tp^{tBu,Me}Cu(NCMe)$ (**1**) was prepared by direct

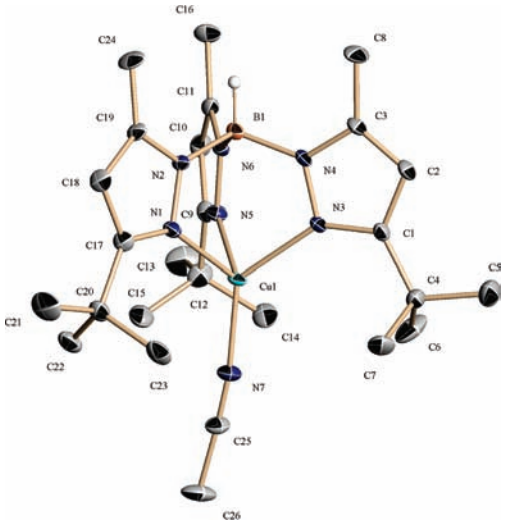

Figure 1. Molecular structure of $Tp^{tBu,Me}Cu(NCMe)$ (**1**) (30% displacement ellipsoids, hydrogen atoms have been omitted except for that bound to the boron atom).

Scheme 3. Synthesis of the Catalyst Precursor $Tp^{tBu,Me}Cu(NCMe)$ (1)

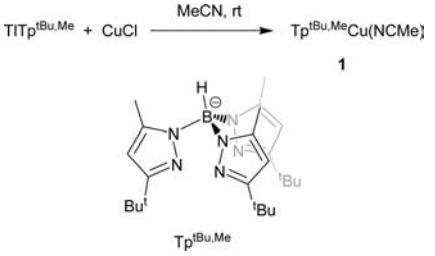

reaction of the thallium salt of the corresponding $Tp^{tBu,Me}$ ligand and copper chloride in acetonitrile as the solvent (Scheme 3). Spectroscopic data were in agreement with the proposed formula. Since the catalytic system studied in this contribution is markedly influenced by the copper species that exists in the reaction mixture, we have carried out X-ray diffraction studies to unambiguously assign the nature of the catalyst precursor. As shown in Figure 1, complex **1** displays a structure that corresponds to a distorted tetrahedron around the metal center with the N−C−Me group slightly displaced from the ideal B−Cu axis. This feature, as well as distances and angles, are quite similar to other already reported $Tp^xCu(NCMe)$[8] complexes and deserve no additional comments.

Once the nature of the precatalyst was established, we studied its behavior in solution. Complex **1** was dissolved in C_6D_6, and the solution was investigated by ^1H NMR. In addition to that of **1**, a second set of resonances corresponding to $[Tp^{tBu,Me}Cu]_2$[9] (**2**) was observed, growing with time although at a very low rate. Figure 2 shows the kinetics of this process, in which acetonitrile dissociates from the copper center with a $k_{obs,init} = 1.43 \times 10^{-4}\ M^{-1}\ s^{-1}$. In order to ascertain if an equilibrium between these acetonitrile adducts and the dimeric $[Tp^xCu]_2$ could exist in solution, 1 equiv of MeCN (referred to Cu) was added to a solution of previously prepared $[Tp^{tBu,Me}Cu]_2$ (**2**). After 100 h at room temperature, the relative concentrations of **1** and **2** were measured by integrating the peaks corresponding to the ^{t}Bu,

dx.doi.org/10.1021/ic102279w |Inorg. Chem. 2011, 50, 2458–2467

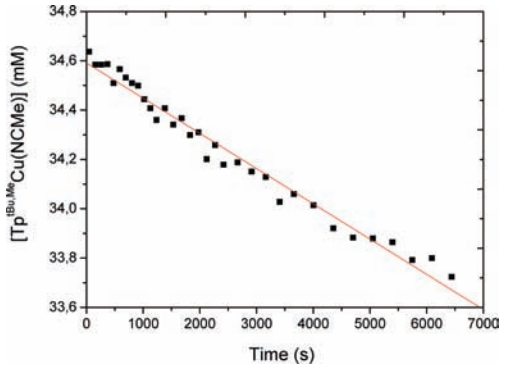

Figure 2. Kinetics of dissociation of acetonitrile from $Tp^{tBu,Me}$-Cu(NCMe) in C_6D_6.

leading to $K_{eq} = 3.2 \times 10^{-2}$ (eq 1).

$$\underset{\mathbf{1}}{Tp^{tBu,Me}Cu(NCMe)} \underset{+CH_3CN}{\overset{-CH_3CN}{\rightleftharpoons}} \underset{\mathbf{2}}{1/2[Tp^{tBu,Me}Cu]_2} \qquad (1)$$

$$K_{ep} = 3.2 \times 10^{-2}$$

It seems reasonable to assume that these transformations occur through the intermediacy of the coordinatively unsaturated species $Tp^{tBu,Me}Cu$ (Scheme 4). In fact, we have recently demonstrated that the olefin exchange processes in $Tp^{x}Cu$(olefin) complexes take place by means of a dissociative mechanism, which involves such $Tp^{x}Cu$ intermediates.[10] The addition of a 10-fold excess of styrene to a solution of complex **1** did not induce the formation of any olefin adduct in detectable amounts in the NMR detection limit. A similar experiment using the dinuclear complex **2** and styrene showed the formation of $Tp^{tBu,Me}Cu$(styrene) (**3**) to some extent. The existing equilibria in solution when complex **1** is dissolved in a styrene solution seem to be those shown in Scheme 4. Slow dissociation of the MeCN takes place to generate $Tp^{tBu,Me}Cu$ that is also in equilibrium with the dinuclear and the styrene complexes **2** and **3**, respectively. In spite of such equilibria, it should be pointed out that this system is quite simple compared with other already described systems for this transformation, in which a copper(I) source and the corresponding ligand are mixed in situ. A very elegant work from Matyjaszewki's group have recently shown[11] that a number of different species with distinct metal-to-ligand ratios are present in solution, therefore affecting the catalytic behavior. In our system, there $Tp^{x}Cu$ unit remains as a core along the reaction time, only one coordination site being available for the catalytic process to occur.

Reaction of the Copper Catalyst Precursor 1 with CCl_4. We have chosen the ATRA reaction of styrene and CCl_4 as the model for this study (eq 2).

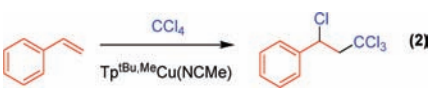

This is the probe reaction commonly employed to test the validity of a given complex as catalyst for this transformation. However, synthetic application using this polyhalomethane reagent in radical addition reactions has been also described.[12] Once the pre-equilibria existing in solutions of complex **1** and styrene (Scheme 4) are established, the reaction with CCl_4 was studied. The stoichiometric [**1**]:[CCl_4] in benzene-d_6 at 30 °C

Scheme 4. Solution Equilibria Involving the Catalyst Precursor $Tp^{tBu,Me}Cu$(NCMe) (1) and Styrene

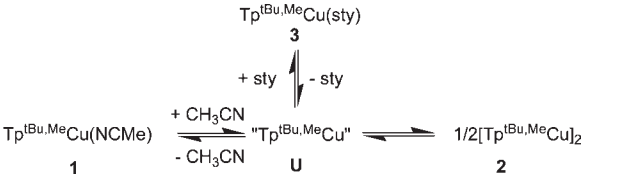

Scheme 5. Equilibria Affecting the Formation of Cu(II) Species

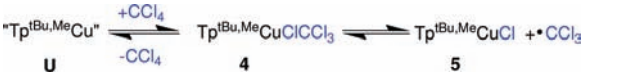

(in the absence of styrene) did not provide any information: after 24 h most of the initial $Tp^{tBu,Me}Cu$(NCMe) remained unreacted. But the use of a 1:200 ratio, for example, a large excess of CCl_4 simulating the catalytic transformation, led to the formation of the Cu(II) complex $Tp^{tBu,Me}CuCl$[9] (**5**) as well as the stoichiometric amount of hexachloroethane, the product resulting from the homocoupling of two $^{\bullet}CCl_3$ radicals (Scheme 5) after 4 h. Interestingly, a second experiment carried out adding 20 equiv of acetonitrile with respect to the catalyst precursor induced a significant decrease in the reaction rate of the formation of complex **5**. Therefore, all these pieces of information seem to favor the existence of an equilibrium between the unsaturated species $Tp^{tBu,Me}Cu$ (**U**) and the CCl_4 adduct $Tp^{tBu,Me}CuClCCl_3$ previously to the formation of the copper(II) chloride complex **5**. The latter step supposes the formation of the $^{\bullet}CCl_3$ radical that undegoes the homocoupling step. It is interesting to note that when styrene is added, that is, under catalytic conditions, hexachloroethane is not observed in the NMR detection limit. The effect of the added acetonitrile is explained by the control exerted in the dissociation equilibrium from the catalyst precursor **1**.

A well-known feature of atom transfer radical reactions is the persistent radical effect. The equilibrium between Cu(I) and Cu(II) species is crucial to control the amount of radicals delivered into the reaction medium and therefore to avoid side, undesired reactions. When the concentration of radicals is maintained at low values, radical-to-radical coupling is minimized and therefore the selectivity toward the desired products (addition of CCl_4 to the C=C bond) is maximized. In our case, the concentration of the Cu(II) species **5** and subsequently the concentration of $^{\bullet}CCl_3$ are controlled by the concentration of the unsaturated intermediate **U**. As explained above, loss of acetonitrile from complex **1** is slow, and because of its dissociative nature, it can be directed with the addition of free MeCN. Overall, in our system the persistent radical effect equilibrium could be written as in eq 3.

$$\underset{\mathbf{1}}{Tp^{tBu,Me}Cu(NCMe)} + CCl_4 \underset{k_{-1}}{\overset{k_1}{\rightleftharpoons}} \underset{\mathbf{5}}{Tp^{tBu,Me}CuCl} + {}^{\bullet}CCl_3 + MeCN \qquad (3)$$

Due to the equilibria shown in Schemes 4 and 5, the concentration of **5** in solution is very low in comparison with that of **1**, particularly when free MeCN is added for such purpose.

In our previous proposal (Scheme 2), we assumed that the Cu(II) complex $Tp^{tBu,Me}CuCl$ (**5**) could be trapped by either the

dx.doi.org/10.1021/ic102279w |*Inorg. Chem.* 2011, 50, 2458–2467

olefin or an added donor, acetonitrile in this case, to give $Tp^{tBu,Me}CuCl(NCMe)$, and that this would be the crucial species to initiate the deactivation step. To test this, we have now studied the solution behavior of complex **5** in the presence and absence of acetonitrile, using toluene as the solvent. Figure 3 shows the UV−vis spectrum of this complex in toluene that did not vary when excess of acetonitrile was added. Therefore, our previous assumption that the pentacoordinated complex $Tp^{tBu,Me}CuCl$-(NCMe) was formed is no longer valid.

Effect of the Variables in the Catalytic Reaction. We have carried out kinetic experiments to study the effect that a variation in [catalyst], [styrene], and $[CCl_4]$ induce in the catalytic reaction. In the first case, as shown in Figure 4, a linear dependence of k_{obs} vs $[\mathbf{1}]_0$ was observed ($[\mathbf{1}]_0$ corresponds to the total concentration of copper species in solution, $[Cu]_{tot}$). A second set of experiments in which styrene concentration was varied (Figure 5) indicated an inhibitory effect of the olefin, as inferred from the decrease of k_{obs} (rate constant for product formation) when increasing [styrene]. Finally, the effect of $[CCl_4]$ led to a saturation curve (Figure 6). We have also analyzed the dependence of the rate on the reaction temperature to estimate the activation parameters for the ATRA reaction of styrene and CCl_4 catalyzed by complex **1**. Figure 7 contains the data collected as an Eyring plot. Good linear correlation analysis, when fitted to the standard Eyring equation, has provided the activation parameters $\Delta H^{\ddagger}$ = 29.6(3) kcal/mol and $\Delta S^{\ddagger}$ = 19.3(2) cal/(mol K), for $\Delta G^{\ddagger}$ = 23.8(5) kcal/mol.

Therefore, any mechanistic proposal should explain the experimental observations, which are (i) linear dependence with catalyst concentration, (ii) inhibitory effect of acetonitrile, (iii) inhibitory effect of [styrene], (iv) saturation effect of $[CCl_4]$, and (v) $\Delta S^{\ddagger} > 0$. The inhibitory effects of both acetonitrile and olefin could be readily explained by the equilibria shown in Scheme 4, the higher the amounts of MeCN and/or styrene in the reaction mixture, and the lower the concentration of $Tp^{tBu,Me}Cu$ (**U**) to react with CCl_4. The saturation effect when increasing $[CCl_4]$ was already observed by Van Koten and coworkers[4c] with nickel-based catalysts; an explanation is yet to be made. The positive value of the activation entropy could be in agreement with the dissociation of acetonitrile from **1** as the rate determining step. In other cases, it has been proposed that the activation step, that leading to the fomation of **5** and the $^{\bullet}CCl_3$ radical, is the rate determining step, through the intermediacy of an adduct-radical.[13] But the formation of the such adduct radical would involve an early transition state more ordered than the reactants, in contrast with that positive entropy parameter.

There is one major issue yet to be evaluated. It is well-known that in these catalytic systems the bimolecular radical coupling originates a secondary effect, the accumulation of Cu(II) species that cannot return to the lower oxidation state. In this manner, the catalyst deactivates with time and conversions are lowered. In order to evaluate such effect, we have monitored by UV−vis the accumulation of Cu(II), in our case, the presence of $Tp^{tBu,Me}$-CuCl (**5**), in solution during the catalytic reaction. The initial [**1**] was 1.4×10^{-3} M, and after 3 min at 20 °C, [**5**] was estimated as 2.0×10^{-4} M. The values at 2.5 and 14 h were 2.3×10^{-4} M, indicating that the Cu(I)−Cu(II) equilibrium is reached in the first stages of the catalytic reaction and that no accumulation takes place (see Supporting Information). The explanation for this behavior should invoke a highly favorable deactivation step in which **5** and the corresponding radical would collapse easily.

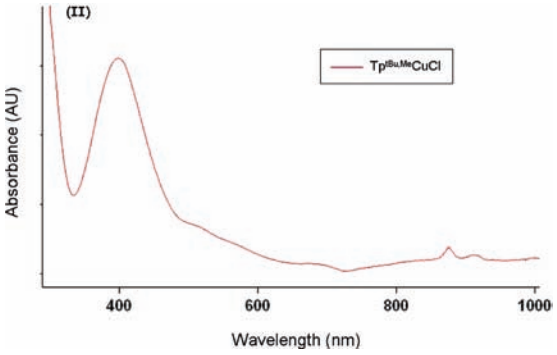

Figure 3. Electronic spectrum of $Tp^{tBu,Me}CuCl$ (**3**) in toluene. Identical wavelengths were observed in the presence as well as in the absence of CH_3CN [398 nm (1532) and 875 nm (68)] [λ nm (ε M^{-1} cm^{-1})].

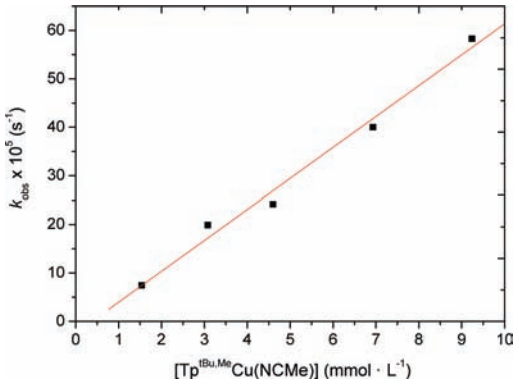

Figure 4. Dependence of k_{obs} with the concentration of the catalyst precursor **1**, for the ATRA reaction of styrene and CCl_4.

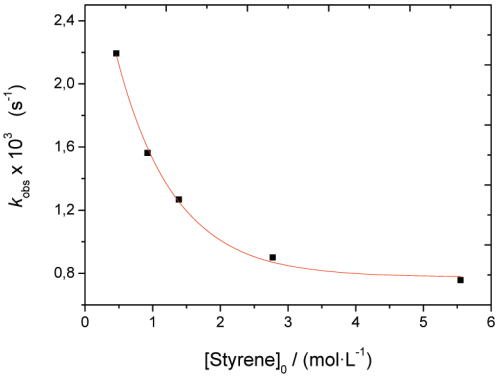

Figure 5. Dependence of k_{obs} for product formation with the olefin concentration for the ATRA reaction of styrene and CCl_4 catalyzed by **1**. Conditions: [cat] = 4.6 mM; solvent, benzene-d_6.

Rate Law. On the basis of the collected data, Scheme 6 shows the different reactions that should be taken into account to explain this transformation. Styrene consumption would be given by

$$-\frac{d[sty]}{dt} = k_2[^{\bullet}CCl_3][sty] \qquad (4)$$

The variation of the concentration of the $^{\bullet}CCl_3$ with time would be

$$-\frac{d[^{\bullet}CCl_3]}{dt} = k_1[\mathbf{4}] - k_{-1}[\mathbf{5}][^{\bullet}CCl_3] - k_2[^{\bullet}CCl_3][sty]$$

dx.doi.org/10.1021/ic102279w |*Inorg. Chem.* 2011, 50, 2458–2467

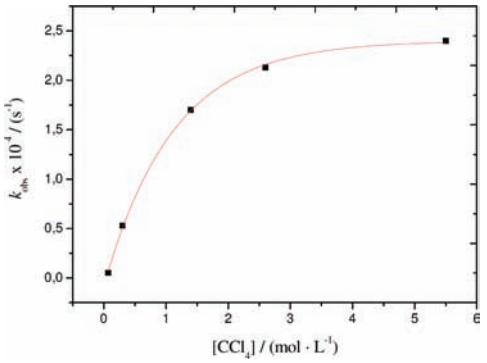

Figure 6. Dependence of k_{obs} with the CCl_4 concentration for the ATRA reaction of styrene and CCl_4 catalyzed by **1**. Conditions: [cat] = 4.6 mM; solvent, benzene-d_6.

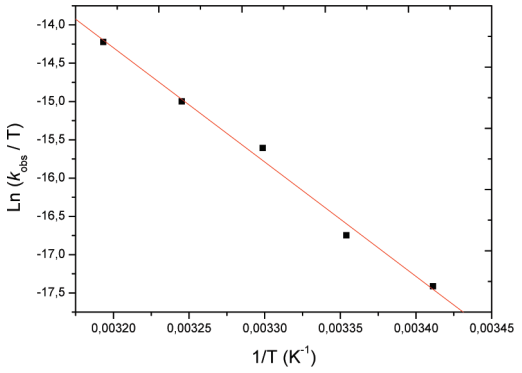

Figure 7. Eyring plot for the ATRA reaction of styrene and CCl_4 catalyzed by **1**. Conditions [**1**]:[styrene]:[CCl_4] = 1:300:1200; [cat] = 1.5 mM; solvent, benzene-d_6.

At this stage, and in order to simplify the kinetic calculations, we propose a first approximation: since the concentration of **5** remains constant along the reaction time, we have assumed steady state conditions for it as well as for $^{\bullet}CCl_3$. Therefore, we assume that

$$-\frac{d[^{\bullet}CCl_3]}{dt} = 0$$

$$k_1[\mathbf{4}] - k_2[^{\bullet}CCl_3][sty] \gg -k_{-1}[\mathbf{5}][^{\bullet}CCl_3]$$

From which the value of [$^{\bullet}CCl_3$] is calculated as

$$[^{\bullet}CCl_3] = \frac{k_1[\mathbf{4}]}{k_2[sty]}$$

And substituting above we end that

$$-\frac{d[sty]}{dt} = k_1[\mathbf{4}]$$

From equilibria we can write

$$K_C = \frac{[\mathbf{4}]}{[\mathbf{U}][CCl_4]} \Rightarrow [\mathbf{4}] = K_C[\mathbf{U}][CCl_4]$$

And substituting above

$$-\frac{d[sty]}{dt} = k_1K_C[\mathbf{U}][CCl_4]$$

Scheme 6. Different Steps in the ATRA Reaction of Styrene and CCl_4 Using Complex 1 as the Catalyst Precursor

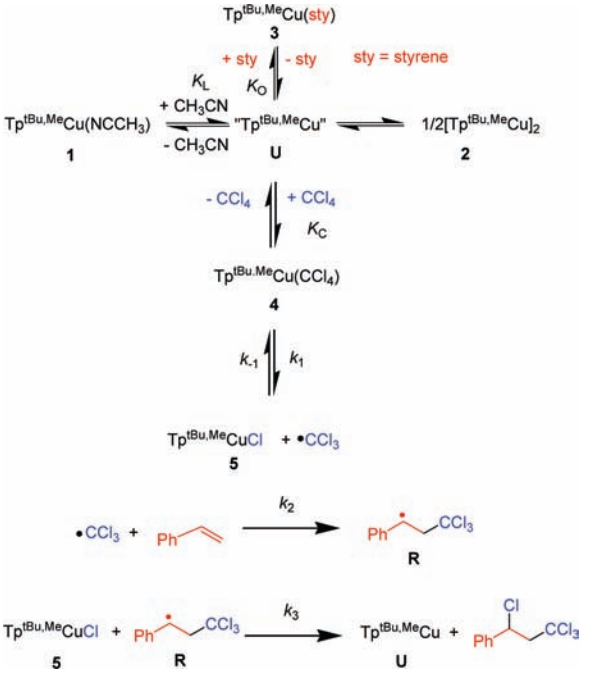

This equation needs to be written as a function of the total Cu concentration, which is the initial concentration of the catalyst precursor **1**. At this stage, we introduce a second assumption: to account for the total concentration of copper species in solution, only the acetonitrile, styrene, and CCl_4 adducts as well as the unsaturated intermediate Tp^{tBu,Me}Cu (**U**) will be considered. The already mentioned steady-state condition for **5** and the experimental data previously commented on showing that, in the presence of acetonitrile or olefin, the dinuclear species **2** does not exist in solution support this second approximation. We could employ the experimental data collected for [**5**] as a fraction of initial [**1**] but will stand on our initial assumption.

$$[Cu]_{tot} \approx [\mathbf{1}] + [\mathbf{3}] + [\mathbf{4}] + [\mathbf{U}]$$

Again, from different equilibria we obtain [**1**], [**3**], and [**4**] as a function of [**U**]:

$$K_L = \frac{[\mathbf{U}][MeCN]}{[\mathbf{1}]} \Rightarrow [\mathbf{1}] = \frac{[\mathbf{U}][MeCN]}{K_L}$$

$$K_O = \frac{[\mathbf{3}]}{[\mathbf{U}][sty]} \Rightarrow [\mathbf{3}] = K_O[\mathbf{U}][sty]$$

$$K_C = \frac{[\mathbf{4}]}{[\mathbf{U}][CCl_4]} \Rightarrow [\mathbf{4}] = K_C[\mathbf{U}][CCl_4]$$

The value for $[Cu]_{tot}$ is therefore given by

$$[Cu]_{tot} = \frac{[\mathbf{U}][MeCN]}{K_L} + [\mathbf{U}] + K_O[\mathbf{U}][sty] + K_C[\mathbf{U}][CCl_4]$$

$$= [\mathbf{U}]\left(\frac{[MeCN]}{K_L} + 1 + K_O[sty] + K_C[CCl_4]\right)$$

dx.doi.org/10.1021/ic102279w |*Inorg. Chem.* 2011, 50, 2458–2467

and

$$[\mathbf{U}] = \frac{[\mathrm{Cu}]_{\mathrm{tot}}}{\frac{[\mathrm{MeCN}]}{K_{\mathrm{L}}} + 1 + K_{\mathrm{O}}[\mathrm{sty}] + K_{\mathrm{C}}[\mathrm{CCl_4}]}$$

Substitution in the equation for styrene consumption provides

$$-\frac{\mathrm{d}[\mathrm{sty}]}{\mathrm{d}t} = \frac{k_1 K_{\mathrm{C}}[\mathrm{CCl_4}][\mathrm{Cu}]_{\mathrm{tot}}}{\frac{[\mathrm{MeCN}]}{K_{\mathrm{L}}} + 1 + K_{\mathrm{O}}[\mathrm{sty}] + K_{\mathrm{C}}[\mathrm{CCl_4}]} \quad (5)$$

Equation 5 shows the rate law obtained under the mechanistic picture shown in Scheme 6, and with the discussed approximations, their validity now depends on its use to explain the experimental results. In this sense, this equation is in very good agreement with all the experimental data available. Thus, the linear dependence with catalyst concentration comes straight from such equation. Similarly, the inhibition of the process in acetonitrile as the solvent as well as the observation of lower reaction rates with added acetonitrile come from an inverse dependence with [MeCN]. At large [MeCN], and given the low value of K_{L}, $[\mathrm{MeCN}]/K_{\mathrm{L}}$ is quite large, leading to no conversion experiments. The same inhibitory effect could be applied to the olefin, since an increase in [sty] would imply a decrease in olefin consumption.

The saturation effect observed at high $[\mathrm{CCl_4}]$ can now be explained in a simple manner: at large values of $[\mathrm{CCl_4}]$ we can assume that

$$\frac{[\mathrm{MeCN}]}{K_{\mathrm{L}}} + 1 + K_{\mathrm{O}}[\mathrm{sty}] + K_{\mathrm{C}}[\mathrm{CCl_4}] \approx K_{\mathrm{C}}[\mathrm{CCl_4}]$$

and hence

$$-\frac{\mathrm{d}[\mathrm{sty}]}{\mathrm{d}t} = \frac{k_1 K_{\mathrm{C}}[\mathrm{CCl_4}][\mathrm{Cu}]_{\mathrm{tot}}}{\frac{[\mathrm{MeCN}]}{K_{\mathrm{L}}} + 1 + K_{\mathrm{O}}[\mathrm{sty}] + K_{\mathrm{C}}[\mathrm{CCl_4}]} = \frac{k_{12} K_{\mathrm{C}}[\mathrm{CCl_4}][\mathrm{Cu}]_{\mathrm{tot}}}{K_{\mathrm{C}}[\mathrm{CCl_4}]} = k_2[\mathrm{Cu}]_{\mathrm{tot}}$$

At the saturation limit, $k_{\mathrm{obs}} = k_2[\mathrm{Cu}]_{\mathrm{tot}}$, and k_1 can be obtained from the flat region of the curve in Figure 6; an estimation of the value of k_1 as 2.4×10^{-4} s^{-1} has been obtained.

In a separate experiment similar to that described by Matyjaszewski and co-workers,[14] **1** was reacted with $\mathrm{CCl_4}$ in the presence of TEMPO (as excess radical trapping agent) to directly obtain the value of k_1, which was found to be 2.0×10^{-4} s^{-1}, in good agreement with the above. We believe that this cross-check experiment assesses the validity of the kinetic study, from which the following mechanistic proposal can be also proposed.

Mechanistic Proposal. On the basis of the previous and new experimental data, Scheme 7 displays a mechanistic proposal for complex **1** as the catalyst precursor. The first step would be the dissociation of the acetonitrile molecule, the presence of added acetonitrile being crucial to regulate the amount of the real catalytic species, $\mathrm{Tp^{tBu,Me}Cu}$, and, subsequently, the concentration of radicals in the reaction mixture. The next step would consist of the interaction of $\mathrm{Tp^{tBu,Me}Cu}$ with $\mathrm{CCl_4}$, in the so-called activation step, that would provide an adduct radical prior to the generation of $\mathrm{Tp^{tBu,Me}CuCl}$ (**5**) and $^{\bullet}\mathrm{CCl_3}$. At this stage, in the nonmetal mediated route, $^{\bullet}\mathrm{CCl_3}$ and styrene would react to give another radical that further reacts with **5** in the final, deactivation step.

Scheme 7. Mechanistic Proposal for the ATRA Reaction Catalyzed by $\mathrm{Tp^xCu(NCMe)}$

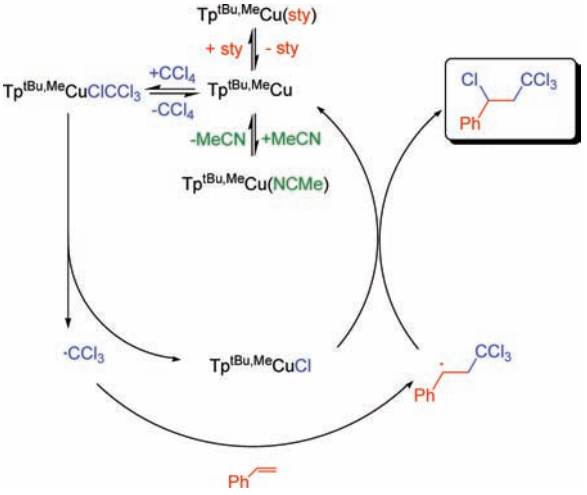

Although the above mechanistic proposal is in agreement with all data collected, we decided to carry out theoretical calculations that provide additional information about the overall mechanistic picture, with particular emphasis in two issues: (a) the rate determining step, which we have located in the dissociation of acetonitrile from complex **1**, and (b) the deactivation step. In the latter case, an alternative explanation would invoke the existence of a pentacoordinated intermediate of composition $\mathrm{Tp^{tBu,Me}Cu(NCMe)Cl}$ due to the trapping of **5** with acetonitrile. Such pentacoordinated intermediate would collapse with the carbon-centered radical $\mathrm{PhCHCH_2CCl_3}$ to afford the final product as well as complex **1** to restart the catalytic cycle.

Theoretical Studies. We first carried out a series of DFT and DFT/MM calculations. We modeled the ATRA of $\mathrm{CCl_4}$ to $\mathrm{C_2H_4}$ catalyzed by $\mathrm{Tp^{tBu,Me}Cu(NCMe)}$ in the presence of MeCN. The resulting potential energy profiles are presented in Figures 8 and 9. The first profile, Figure 8, deals with the equilibria related to ligand exchange at the copper center prior to the C−Cl bond cleavage. In the presence of three potential ligands, as MeCN, $\mathrm{C_2H_4}$, and $\mathrm{CCl_4}$, there is an equilibrium between four Cu(I) species: the three-coordinate complex $\mathrm{Tp^{tBu,Me}Cu}$ (**U**) and the four-coordinate species $\mathrm{Tp^{tBu,Me}Cu(NCMe)}$ (**1**), $\mathrm{Tp^{tBu,Me}Cu(C_4H_4)}$, and $\mathrm{Tp^{tBu,Me}Cu(CCl_4)}$ (**4**). The acetonitrile adduct **1** produces the most stable species in this context and will be used as origin of energies for all compounds discussed. This $\mathrm{Tp^{tBu,Me}Cu(NCMe)}$ species is followed in stability by the complexes with $\mathrm{C_2H_4}$ and $\mathrm{CCl_4}$, 9.8 and 14.1 kcal mol^{-1} above, respectively. The highest energy corresponds to the three-coordinate complex $\mathrm{Tp^{tBu,Me}Cu}$, 21.5 kcal mol^{-1} above the MeCN complex. All these complexes hold fully occupied metal d orbitals ($\mathrm{d^{10}}$). Therefore, the four-coordinate complexes are 18-electron species, and all ligand exchange reactions proceed likely by a dissociative mechanism, going through $\mathrm{Tp^{tBu,Me}Cu}$. This is in agreement with previous experimental and theoretical studies from these laboratories with $\mathrm{Tp^xCu(olefin)}$ complexes.[10] The relatively high energy of $\mathrm{Tp^{tBu,Me}Cu}$, 21.5 kcal mol^{-1} above the $\mathrm{Tp^{tBu,Me}Cu(NCMe)}$, is the first barrier that must be overcome for the catalytic cycle to proceed. It is worth mentioning that the $\mathrm{Tp^{tBu,Me}Cu(CCl_4)}$ complex, the one that will open the reaction channel for the ATRA process, is less stable than the MeCN and $\mathrm{C_2H_4}$ counterparts. This is in agreement with the

dx.doi.org/10.1021/ic102279w |Inorg. Chem. 2011, 50, 2458–2467

experimental observation that an increase in either acetonitrile or olefin can slow down the overall process.

The second computed profile, Figure 9, shows the reaction from the $Tp^{tBu,Me}Cu(CCl_4)$ complex to the final products. This starting species may be seen as a $Tp^{tBu,Me}CuCl{-}CCl_3$ adduct, because only one of the chlorine atoms of CCl_4 is interacting with copper. The Cu−Cl distance is quite long, 2.609 Å. Homolytic cleavage of the C−Cl bond produces the species $[Tp^{tBu,Me}CuCl]...[^{\bullet}CCl_3]$, a Cu(II) complex at the C−Cl bond dissociation limit, which is about 7.0 kcal mol^{-1} above the $Tp^{tBu,Me}CuCl\text{-}CCl_3$ intermediate. At the beginning of the C−Cl bond cleavage, the spin density on each atomic center is zero but spin localization develops as the homolytic cleavage advances toward the two separate doublet systems. The dissociated $^{\bullet}CCl_3$ radical can attack the olefin with a low barrier of 5.7 kcal mol^{-1} and an exothermicity of −17.8 kcal mol^{-1} (not shown in the profile). The resulting $^{\bullet}CH_2CH_2CCl_3$ radical rejoins then the energy profile in Figure 9 to yield the product. We have considered two possibilities: this new radical can either attack directly the $Tp^{tBu,Me}CuCl$ intermediate or attack a pentacoordinate $Tp^{tBu,Me}CuCl(NCMe)$ species that may be formed in solution, as a bifurcation shown in the profile. The direct reaction between the radical and the four-coordinate Cu(II) intermediate is barrierless in terms of potential energy, while the reaction through the five-coordinate intermediate goes through an additional barrier of 6.4 kcal mol^{-1}. Therefore, the five-coordinate species with chloride and acetonitrile simultaneously bonded to a copper(II) center should not be formed, in good agreement with the UV−vis studies. The reaction will therefore proceed through attack of the organic radical on the $Tp^{tBu,Me}CuCl$ complex, in an exothermic step by 30.1 kcal mol^{-1}.The slightly endothermic (10.3 kcal mol^{-1}) separation of the product will then yield the $Tp^{tBu,Me}Cu$ complex, which can reinitiate the catalytic cycle upon carbon tetrachloride coordination, or it can coordinate again acetonitrile or olefin and re-enter the equilibria described in Figure 8.

The computed energy profiles confirm the validity of the mechanistic proposal in Scheme 7 and add further details on the catalytic cycle. The three-coordinate $Tp^{tBu,Me}Cu(I)$ intermediate is the species with the highest energy in the whole process, and its formation is the key for the reaction rate.

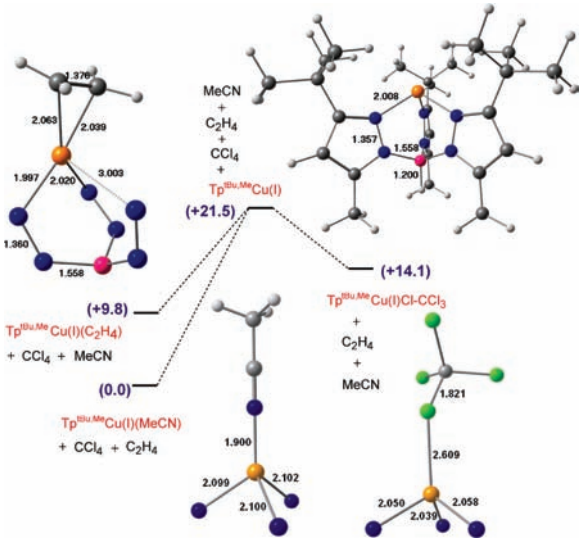

Figure 8. Potential energy diagram for the equilibria connecting the initial form of the catalyst with the reaction channel (energy values are in kcal mol^{-1} and spin densities at selected atoms are shown in italics).

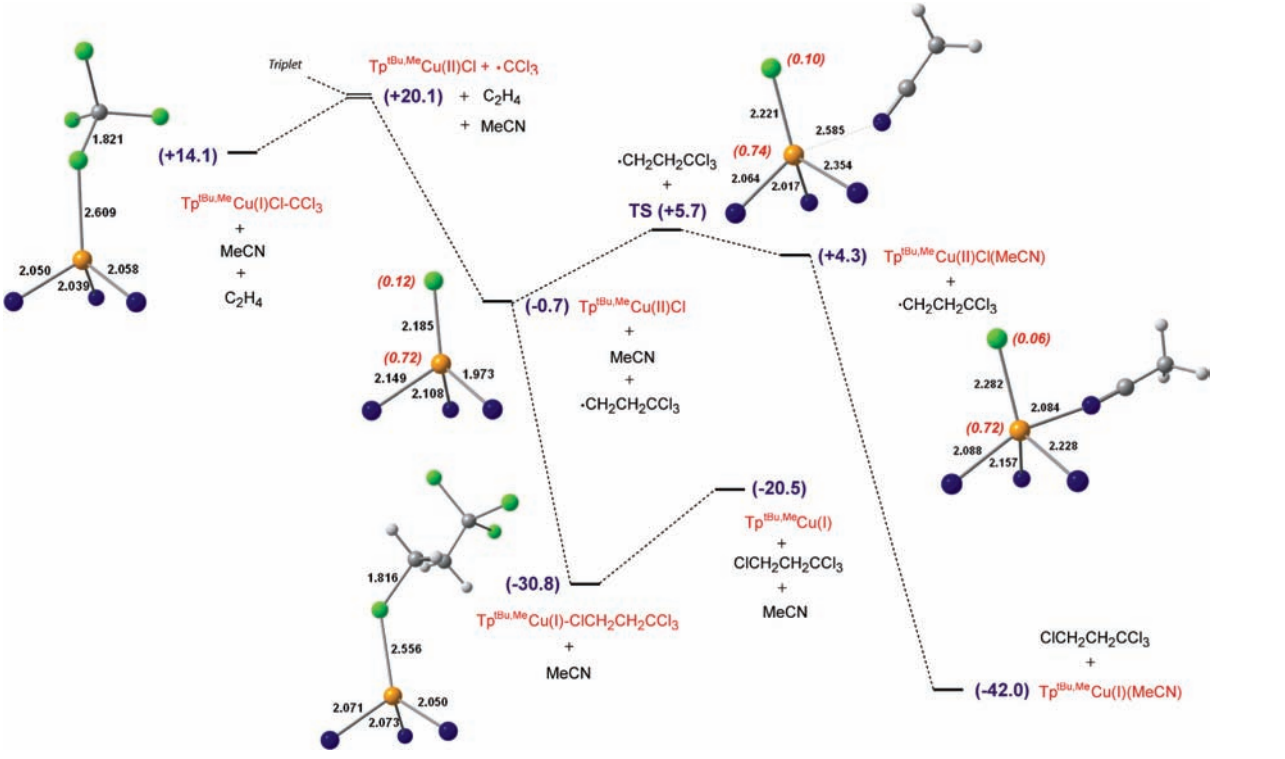

Figure 9. Potential energy diagram for the ATRA of CCl_4 to C_2H_4 by the $Tp^{tBu,Me}Cu(I)$ complex. (Energy values are in kcal mol^{-1}, and spin densities at selected atoms are shown in italics.)

dx.doi.org/10.1021/ic102279w |Inorg. Chem. 2011, 50, 2458–2467

The presence in excess of coordinating agents such as acetonitrile or olefin will reduce the concentration of this high energy intermediate and can thus slow down the reaction. The $Tp^{tBu,Me}Cu(II)Cl$ intermediate will necessarily have a low concentration, because it reacts without barrier with the coexisting radical species in solution, thus confirming the validity of the rate law presented above.

CONCLUSIONS

A complete mechanistic proposal for the model Atom Transfer Radical Addition of CCl_4 to styrene using $Tp^{tBu,Me}Cu(NCMe)$ as the catalyst precursor has been made. The importance of several equilibria between Cu(I) species to control the amount of the real catalytic species has been established. This seems crucial since that concentration directly affects the concentration of radicals in solution and, when in the appropriate range, allows the process to be directed toward the desired product and, subsequently, avoids the formation of other nondesired products derived from radical coupling reactions.

EXPERIMENTAL SECTION

General Information. All preparations were carried out in a glovebox, placed into a thick walled pressure NMR tube, and sealed with a Teflon screw cap under nitrogen. Starting materials and reagents were purchased from Aldrich and were purified as follows: carbon tetrachloride was distilled, and styrene was filtered on alumina columns prior to use. The homoscorpionate ligand[15,16] and the $[Tp^{tBu,Me}Cu]_2$[9] (**2**) complex were prepared according to literature methods. NMR experiments were run in a Varian Mercury 400 MHz spectrometer. UV−vis spectra were recorded in a 1 cm quartz cuvette under nitrogen using a Cary 50 UV/vis spectrophotometer (Varian Scientific Instruments).

Synthesis of the Complex $Tp^{tBu,Me}Cu(NCMe)$ (1). $TlTp^{tBu,Me}$ (0.81 mmol) and cuprous chloride, CuCl (0.82 mmol), were stirred in CH_3CN (20 mL) for 1 h. The mixture was filtered, and the colorless solution was concentrated under vacuum and cooled at −20 °C to give a white crystalline solid of composition $Tp^{tBu,Me}Cu(NCMe)$ in 80% yield. ^1H NMR (400 MHz, C_6D_6) δ = 0.86 (br s, 3 H), 1.59 (s, 27 H), 2.35 (s, 9 H), 5.85 ppm (s, 3H); ^{13}C NMR (100 MHz, C_6D_6) δ = 2.5, 12.4, 31.2, 103.2, 144.5, 163.5 ppm. IR (Nujol) ν(CN) = 2206, ν(B−H) = 2369 cm^{-1}. For crystallographic data of **1** see Supporting Information.

Reaction of 1 with CCl_4. A toluene solution (30 mL) of complex **1** (0.13 mmol) and CCl_4 (200 mmol) was stirred for 4 h. A red brown solution was obtained. The volatiles were removed under vacuum, and the residue was extracted with diethyl ether. The resulting solution was concentrated under reduced pressure. Crystallization at −30 °C afforded a red crystalline solid, for which the IR, NMR, and analytical data were identical to those reported for $Tp^{tBu,Me}CuCl$.[9]

Kinetic Study of the Dissociation of Acetonitrile from 1. A total of 2.01×10^{-2} mmol of **1** were dissolved in C_6D_6 (0.6 mL), transferred into a pressure NMR tube, and sealed with a Teflon screw cap. The relative concentrations of **1** and **2** were monitored by ^1H NMR at 298 K with time using the resonances corresponding to the ^{t}Bu.

Equilibrium Constant Measurement. To solution of 15 mg (1.50×10^{-2} mmol) of **2** in C_6D_6 (0.6 mL), 1 equiv of CH_3CN and 1 equiv of biphenyl, as internal standard, were added. The mixture was transferred into a pressure NMR tube and sealed with a Teflon screw cap. The relative concentrations of **1** and **2** were measured by integrations of the resonances corresponding to the ^{t}Bu protons of each compound, after 100 h, when the equilibrium was reached.

Kinetics of ATRA of CCl_4 to Styrene at Different Temperatures. A mixture of styrene (0.84 mmol), complex **1** (2.8×10^{-3} mmol from a stock solution), and CCl_4 (9.3 mmol) was dissolved in the required amount of C_6D_6 to a total volume of 1.86 mL; [catalyst] = 1.5 mM. The solution was transferred into a pressure NMR tube and sealed with a Teflon screw cap. The tube was removed from the glovebox and placed in an oil bath. The temperature was controlled in the range 10−50 °C (±0.1 °C). The conversions were monitored by ^1H NMR spectroscopy at the desired times. The Eyring plot for the reactions are given in Figure 7. Activation parameters were calculated over the temperature range from the least-squares fit of values of $\ln(k/T)$ to $1/T$, according to the equation

$$\ln\left(\frac{k}{T}\right) = \ln\left(\frac{k_B}{h}\right) + \frac{\Delta S^{\ddagger}}{R} + \frac{\Delta H^{\ddagger}}{RT}$$

Kinetics of the Reaction of CCl_4 to Styrene at Different CCl_4 Concentrations. Complex **1** (4.1×10^{-3} mmol from a stock solution), styrene (300 equiv, 1.23 mmol), and the desired amount of CCl_4 (10, 60, 300, 600, and 1200 equiv, respectively) were dissolved in the required amount of C_6D_6 to reach a total volume of 900 μL. These five solutions were transferred into pressure NMR tubes and sealed with Teflon screw caps. The conversions were monitored by ^1H NMR spectroscopy.

Kinetics of the Reaction of CCl_4 to Styrene at Different Olefin Concentrations. Complex **1** (4.1×10^{-3} mmol from a stock solution), CCl_4 (3000 equiv, 12.3 mmol), and the desired amount of styrene (100, 200, 300, 600, and 1200 equiv with respect to catalyst) were dissolved in the required amount of C_6D_6 to reach a total volume of 900 μL. The solutions were transferred into five pressure NMR tubes and sealed with Teflon screw caps. The conversions were monitored by ^1H NMR spectroscopy.

Kinetics of the Reaction of CCl_4 to Styrene at Different Catalyst Concentrations. Complex **1** (33, 66, 100, 150, and 200 μL from a 0.05 M stock solution), styrene (1.23 mmol), and CCl_4 (4.92 mmol) were dissolved in the required amount of C_6D_6 to complete a total volume of 900 μL. The solutions were transferred into five pressure NMR tubes and sealed with Teflon screw caps. The conversions were monitored by ^1H NMR spectroscopy.

Alternative Determination of k_1 Using TEMPO. Complex **1** ($2{,}76 \times 10^{-2}$ mmol) and TEMPO (3.6×10^{-2} mmol) were dissolved in 5 mL of deoxygenated toluene in a Schlenk flask. After stirring for 30 min at 30 °C, 1 mL of deoxygenated CCl_4 (6×10^{-4} mmol) and biphenyl (6×10^{-4} mmol) toluene stock solution were added to the Schlenk flask via a degassed syringe. A sample was taken immediately for the reference, and other samples were taken at timed intervals to measure kinetics. The samples were passed through alumina to remove the catalyst. The composition of the samples was analyzed by gas chromatography with a Varian GC-3900 chromatograph with a flame ionization detector.

Computational Details. Gas phase optimizations were carried out using the ONIOM(QM:MM) approach[17] as implemented in the Gaussian03 package.[18] In the ONIOM approach, the full system is divided into two different regions; the electronically sophisticated environment, Cu center, and Tp^H are treated with density functional theory (DFT), while the $-^t$Bu and −Me substituents of $Tp^{tBu,Me}$ are treated with the MM approach. For the QM part, the PBE1PBE functional was applied.[19] The SDD basis set and associated effective core potential with a single f polarization function was used for Cu;[20] the TZVP basis set was considered for all atoms bonded to Cu, and TZV was used for other atoms.[21] UFF[22] was employed in the MM region. All geometry optimizations were full with no restrictions, and vibrational frequency calculations were also performed to establish that the stationary points were minima or transition states. All energies presented are potential energies.

X-ray Crystal Structure Analysis of 1. A single crystal of **1** of suitable size was mounted on a glass fiber using perfluoropolyether oil (FOMBLIN 140/13, Aldrich) in the cold N_2 stream of a low-temperature device attachment. Full crystallographic data and structure refinement are given in the Supporting Information. Intensity data were performed on a Bruker-AXS X8 Kappa diffractometer equipped with an Apex-II CCD area detector, using a graphite monochromator Mo Kα_1 (λ = 0.71073 Å) and a Bruker Cryo-Flex low-temperature device.

dx.doi.org/10.1021/ic102279w |Inorg. Chem. 2011, 50, 2458–2467

The data collection strategy used in all instances was phi and omega scans with narrow frames. Instrument and crystal stability were evaluated from the measurement of equivalent reflections at different measuring times, and no decay was observed. The data were reduced (SAINT)[23] and corrected for Lorentz and polarization effects, and a semiempirical absorption correction was applied (SADABS).[24] The structure was solved by direct methods (SIR-2002)[25] and refined against all F^2 data by full-matrix least-squares techniques (SHELXTL-6.14)[26] minimizing $w[F_o^2 - F_c^2]^2$. All the non-hydrogen atoms were refined with anisotropic displacement parameters. The hydrogen atoms were introduced into the geometrically calculated positions and refined riding on the corresponding parent atoms.

Crystal Data for 1. $C_{28}H_{46}BCuN_8$, M_w = 569.08, colorless prism crystal of dimensions 0.50 × 0.39 × 0.32 mm^3, monoclinic, space group $P2_1/c$, a = 25.0527(14) Å, b = 15.5161(9) Å, c = 17.9635(9) Å, α = 90°, β = 110.9970(10)°, γ = 90°, V = 6519.1(6) Å^3, T = 173(2) K, Z = 8, D = 1.160 Mg/m^3, ρ = 0.699 mm^{-1}, $F(000)$ = 2432; 134670 reflections measured, of which 19771 were unique (R_{int} = 0.0618), 769 refined parameters, final R_1 = 0.0598 for reflections with $I > 2\sigma(I)$, wR_2 = 0.1521 (all data), GOF = 1.084. Final largest diffraction peak and hole: 1.590 and −1.029 e·Å^{-3}. See Supporting Information for supplementary crystallographic data.

■ ASSOCIATED CONTENT

Supporting Information. NMR data for the products, NMR spectra of reaction mixtures, and kinetic plots (PDF) and CIF file. This material is available free of charge via the Internet at http://pubs.acs.org. CCDC 775708 contains the supplementary crystallographic data for the compounds described in this paper. These data can be obtained free of charge via www.ccdc.cam.ac.uk/conts/retrieving.html (or from the Cambridge Crystallographic Data Centre, 12 Union Road, Cambridge CB21EZ, UK; fax +44 1223-336-033; or deposit@ccdc.cam.ac.uk).

■ AUTHOR INFORMATION

Corresponding Author

*E-mail: trodri@dqcm.uhu.es (T.R.B.) and perez@dqcm.uhu.es (P.J.P.).

■ ACKNOWLEDGMENT

We thank the MICINN (Grants CTQ2008-00042BQU, CTQ2008-06866-CO2-02/BQU, and Consolider Ingenio 2010 CSD2006-0003) and the Junta de Andalucía (Proyecto P07-FQM-02794) for financial support.

■ REFERENCES

(1) (a) Kharasch, M. S.; Jensen, E. V.; Urry, W. H. *Science* **1945**, *102*, 128–128. (b) Kharasch, M. S.; Urry, W. H.; Jensen, E. V. *J. Am. Chem. Soc.* **1945**, *67*, 1626–1626.

(2) (a) Eckenhoff, W. T.; Pintauer, T. *Catal. Rev.* **2010**, *52*, 1–59. (b) Pintauer, T.; Matyjaszewski, K. *Chem. Soc. Rev.* **2008**, *37*, 1087–1097. (c) Severin, K. *Curr. Org. Chem.* **2006**, *10*, 217–224. (d) Delaude, L.; Demonceau, A.; Noels, A. F. *Top. Organomet. Chem.* **2004**, *11*, 155–171. (e) Clark, A. J. *Chem. Soc. Rev.* **2002**, *31*, 1–11. (f) Kobrakov, K. I.; Ivanov, A. V. *J. Heterocycl. Chem.* **2001**, *37*, 529–539. (g) Gossage, R. A.; van de Kuil, L. A.; van Koten, G. *Acc. Chem. Res.* **1998**, *31*, 423–431. (h) Iqbal, J.; Bhatia, B.; Nayyar, N. K. *Chem. Rev.* **1994**, *94*, 519–564. (i) Minisci, F. *Acc. Chem. Res.* **1975**, *8*, 165–171.

(3) (a) Matsumoto, H.; Nakano, T.; Nagai, Y. *Tetrahedron Lett.* **1973**, *51*, 5147–5150. (b) Quebatte, L.; Solari, E.; Scopelliti, R.; Severin, K. *Organometallics* **2005**, *24*, 1404–1406. (c) Quebatte, L.; Scopelliti, R.; Severin, K. *Angew. Chem., Int. Ed.* **2004**, *43*, 1520–1524. (d) Simal, F.; Wlodarczak, L.; Demonceau, A.; Noels, A. F. *Eur. J. Org. Chem.* **2001**, 2689–2695. (e) Simal, F.; Wlodarczak, L.; Demonceau, A.; Noels, A. F. *Tetrahedron Lett.* **2000**, *41*, 6071–6074. (f) Tutusaus, O.; Delfosse, S.; Demonceau, A.; Noels, A. F.; Viñas, C.; Teixidor, F. *Tetrahedron Lett.* **2003**, *44*, 8421–8425. (g) Tutusaus, O.; Viñas, C.; Núñez, R.; Teixidor, F.; Demonceau, A.; Delfosse, S.; Noels, A. F.; Mata, I.; Molins, E. *J. Am. Chem. Soc.* **2003**, *125*, 11830–11831. (h) de Clercq, B.; Verpoort, F. *Tetrahedron Lett.* **2002**, *43*, 4687–4690. (i) Wolf, J.; Thommes, K.; Briel, O.; Scopelliti, R.; Severin, K. *Organometallics* **2008**, *27*, 4464–4474. (j) Lundgren, R. J.; Rankin, M. A.; McDonald, R.; Stradiotto, M. *Organometallics* **2008**, *27*, 254–258. (k) Dutta, B.; Solari, E.; Scopelliti, R.; Severin, K. *Organometallics* **2008**, *27*, 423–429. (l) Borguet, Y.; Richel, A.; Delfosse, S.; Leclerc, A.; Delaude, L.; Demonceau, A. *Tetrahedron Lett.* **2007**, *48*, 6334–6338. (m) Motoyama, Y.; Hanada, S.; Shimamoto, K.; Nagashima, H. *Tetrahedron* **2006**, *62*, 2779–2788. (n) Motoyama, Y.; Hanada, S.; Niibayashi, S.; Shimamoto, K.; Takaoka, N.; Nagashima, H. *Tetrahedron* **2005**, *61*, 10216–10226. (o) Quebatte, L.; Haas, M.; Solari, E.; Scopelliti, R.; Nguyen, Q. T.; Severin, K. *Angew. Chem., Int. Ed.* **2005**, *44*, 1084–1088. (p) Quebatte, L.; Scopelliti, R.; Severin, K. *Eur. J. Inorg. Chem.* **2005**, 3353–3358. (q) Fernández-Zúmel, M. A.; Thommes, K.; Kiefer, G.; Sienkiewicz, A.; Pierzchala, K.; Severin, K. *Chem.—Eur. J.* **2009**, *15*, 11601–11607.

(4) (a) Sasson, Y.; Rempel, G. L. *Synthesis* **1975**, 448–450. (b) Grove, D. M.; Van Koten, G.; Verschuuren, A. H. M. *J. Mol. Catal.* **1988**, *45*, 169–174. (c) van de Kuil, L. A.; Grove, D. M.; Gossage, R. A.; Zwikker, J. W.; Jenneskens, L. W.; Drenth, W.; van Koten, G. *Organometallics* **1997**, *16*, 4985–4994.

(5) (a) Pintauer, T. *Eur. J. Inorg. Chem.* **2010**, 2449–2460. (b) Eckenhoff, W. T.; Garrity, S. T.; Pintauer, T. *Eur. J. Inorg. Chem.* **2008**, 563–571. (c) Balili, M. N. C.; Pintauer, T. *Inorg. Chem.* **2009**, *48*, 9018–9026. (d) Eckenhoff, W. T.; Pintauer, T. *Inorg. Chem.* **2007**, *46*, 5844–5846. (e) Pintauer, T.; Eckenhoff, W. T.; Ricardo, C.; Balili, M. N. C.; Biernesser, A. B.; Noonan, S. J.; Taylor, M. J. W. *Chem.—Eur. J.* **2009**, *15*, 38–41.

(6) (a) Muñoz-Molina, J. M.; Belderrain, T. R.; Pérez, P. J. *Inorg. Chem.* **2010**, *49*, 642–645. (b) Muñoz-Molina, J. M.; Caballero, A.; Diaz-Requejo, M. M.; Trofimenko, S.; Belderrain, T. R.; Pérez, P. J. *Inorg. Chem.* **2007**, *46*, 7725–7730.

(7) Muñoz-Molina, J. M.; Belderrain, T. R.; Pérez, P. J. *Adv. Synth. Catal.* **2008**, *350*, 2365–2372.

(8) (a) Fujisawa, K.; Ono, T.; Ishikawa, Y.; Amir, N.; Miyashita, Y.; Okamoto, K.-i.; Lehnert, N. *Inorg. Chem.* **2006**, *45*, 1698–1713. (b) Yap, G. P. A.; Jove, F.; Urbano, J.; Alvarez, E.; Trofimenko, S.; Díaz-Requejo, M. M.; Pérez, P. J. *Inorg. Chem.* **2007**, *46*, 780–787. (c) Schneider, J. L.; Carrier, S. M.; Ruggiero, C. E.; Young, V. G., Jr.; Tolman, W. B. *J. Am. Chem. Soc.* **1998**, *120*, 11408–11418.

(9) Yoon, K.; Parkin, G. *Polyhedron* **1995**, *14*, 811–821.

(10) Martín, C.; Muñoz-Molina, J. M.; Locati, A.; Alvarez, E.; Maseras, F.; Belderrain, T. R.; Pérez, P. J. *Organometallics* **2010**, *29*, 3481–3489.

(11) Bartolomei, N.; Isse, A. A.; Di Marco, V. B.; Gennaro, A.; Matyjaszewski, K. *Macromolecules* 2010, *43*, 9257–9267.

(12) Yoshimitsu, T.; Nakajima, H.; Nagaoka, H. *Tetrahedron Lett.* **2002**, *43*, 8587.

(13) Nondek, L.; Hun, L.-G.; Wichterlová, B.; Krupicka, S. *J. Mol. Catal.* **1987**, *42*, 51.

(14) Matyjaszewski, K.; Paik, H.-J.; Zhou, P.; Diamanti, S. J. *Macromolecules* **2001**, *34*, 5125.

(15) Trofimenko, S. *Scorpionates: The Coordination Chemistry of Polypyrazolylborate Ligands*; Imperial College Press: River Edge, NJ, 1999.

(16) Pettinari, C. *Scorpionates II: Chelating Borate Ligands*; Imperial College Press: River Edge, NJ, 2008.

(17) (a) Maseras, F.; Morokuma, K. *J. Comput. Chem.* **1995**, *16*, 1170–1179. (b) Dapprich, S.; Komaromi, I.; Byun, K. S.; Morokuma, K.; Frisch, M. J. *J. Mol. Struct. (Theochem)* **1999**, *461*, 1–21.

(18) Frisch, M. J.; Trucks, G. W.; Schlegel, H. B.; Scuseria, G. E.; Robb, M. A.; Cheeseman, J. R.; Montgomery, J. J. A.; Vreven, T.; Kudin,

K. N.; Burant, J. C.; Millam, J. M.; Iyengar, S. S.; Tomasi, J.; Barone, V.; Mennucci, B.; Cossi, M.; Scalmani, G.; Rega, N.; Petersson, G. A.; Nakatsuji, H.; Hada, M.; Ehara, M.; Toyota, K.; Fukuda, R.; Hasegawa, J.; Ishida, M.; Nakajima, T.; Honda, Y.; Kitao, O.; Nakai, H.; Klene, M.; Li, X.; Knox, J. E.; Hratchian, H. P.; Cross, J. B.; Bakken, V.; Adamo, C.; Jaramillo, J.; Gomperts, R.; Stratmann, R. E.; Yazyev, O.; Austin, A. J.; Cammi, R.; Pomelli, C.; Ochterski, J. W.; Ayala, P. Y.; Morokuma, K.; Voth, G. A.; Salvador, P.; Dannenberg, J. J.; Zakrzewski, V. G.; Dapprich, S.; Daniels, A. D.; Strain, M. C.; Farkas, O.; Malick, D. K.; Rabuck, A. D.; Raghavachari, K.; Foresman, J. B.; Ortiz, J. V.; Cui, Q.; Baboul, A. G.; Clifford, S.; Cioslowski, J.; Stefanov, B. B.; Liu, G.; Liashenko, A.; Piskorz, P.; Komaromi, I.; Martin, R. L.; Fox, D. J.; Keith, T.; Al-Laham, M. A.; Peng, C. Y.; Nanayakkara, A.; Challacombe, M.; Gill, P. M. W.; Johnson, B.; Chen, W.; Wong, M. W.; Gonzalez, C.; Pople, J. A. *Gaussian03*, Revision C.02; Gaussian, Inc.: Wallingford, CT, 2004.

(19) (a) Perdew, J. P.; Burke, K.; Ernzerhof, M. *Phys. Rev. Lett.* **1996**, *77*, 3865–3868. (b) Adamo, C.; Barone, V. *J. Chem. Phys.* **1999**, *110*, 6158–6159.

(20) Andrae, D.; Haussermann, U.; Dolg, M.; Stoll, H.; Preuss, H. *Theor. Chim. Acta* **1990**, *77*, 123–141.

(21) Schaefer, A.; Huber, C.; Ahlrichs, R. *J. Chem. Phys.* **1994**, *100*, 5829–5835.

(22) Rappé, A. K.; Casewit, C. J.; Colwell, K. S.; Goddard, W. A., III; Skiff, W. M. *J. Am. Chem. Soc.* **1992**, *114*, 10024–10035.

(23) *SAINT+*, Bruker-APEX 2 package, Version 2.1; Bruker Analytical X-ray Solutions: Madison, WI, 2006.

(24) *SADABS*, Bruker-APEX 2 package, Version 2.1; Bruker Analytical X-ray Solutions: Madison, WI, 2006.

(25) Burla, M. C.; Camalli, M.; Carrozzini, B.; Cascarano, G. L.; Giacovazzo, C.; Polidori, G.; Spagna, R. *J. Appl. Crystallogr.* **2003**, *36*, 1103.

(26) *SHELXTL 6.14*; Bruker AXS, Inc.: Madison, WI, 2000−2003.